J. Neurovirol. (2011) 17:201–211
DOI 10.1007/s13365-011-0024-7

Cytomegalovirus-induced sensorineural hearing loss with persistent cochlear inflammation in neonatal mice

Scott J. Schachtele · Manohar B. Mutnal · Mark R. Schleiss · James R. Lokensgard

Received: 22 December 2010 / Revised: 25 February 2011 / Accepted: 2 March 2011 / Published online: 18 March 2011

Abstract Congenital cytomegalovirus (CMV) infection is the leading cause of sensorineural hearing loss (SNHL) in children. During murine (M)CMV-induced encephalitis, the immune response is important for both the control of viral dissemination and the clearance of virus from the brain. While the importance of CMV-induced SNHL has been described, the mechanisms surrounding its pathogenesis and the role of inflammatory responses remain unclear. This study presents a neonatal mouse model of profound SNHL in which MCMV preferentially infected both cochlear perilymphatic epithelial cells and spiral ganglion neurons. Interestingly, MCMV infection induced cochlear hair cell death by 21 days post-infection, despite a clear lack of direct infection of hair cells and the complete clearance of the virus from the cochlea by 14 dpi. Flow cytometric, immunohistochemical, and quantitative PCR analysis of MCMV-infected cochlea revealed a robust and chronic inflammatory response, including a prolonged increase in reactive oxygen species production by infiltrating macrophages. These data support a pivotal role for inflammation during MCMV-induced SNHL.

S. J. Schachtele · M. B. Mutnal · J. R. Lokensgard
Center for Infectious Diseases and Microbiology Translational Research, Department of Medicine, University of Minnesota, Minneapolis, MN, USA

M. R. Schleiss
Center for Infectious Diseases and Microbiology Translational Research, Department of Pediatrics, University of Minnesota, Minneapolis, MN, USA

J. R. Lokensgard (✉)
3-430 Translational Research Facility, University of Minnesota, Minneapolis, MN 55455, USA
e-mail: loken006@umn.edu

Keywords Cytomegalovirus · SNHL · Hearing · Cochlea · Inflammation · Reactive oxygen species

Introduction

Cytomegalovirus (CMV) is the most significant cause of developmental disorders related to intrauterine infection in humans, potentially resulting in mental retardation, epilepsy, microcephaly, hydrocephalus, and hearing loss (Cheeran et al. 2009a) . Sensorineural hearing loss (SNHL) is estimated to account for between 10% and 60% of all nonhereditary congenital SNHL in children. While symptomatic congenitally infected infants have a wide range of disabilities and can be readily identified at birth, SNHL may be the only long-term manifestation of congenital CMV infection in asymptomatic infants. Hence, it is insidious in nature and difficult to identify but nonetheless causes much disability. Although it is clear that CMV infection is involved in congenital SNHL, the mechanisms of pathogenesis are still unknown.

The neonatal mouse central nervous system and peripheral auditory organs are immature at birth, resembling those of a 15-week-old human fetus (Otis and Brent 1954). Mouse models using murine (M)CMV infection (Staczek 1990) are useful because peripheral and intracranial MCMV infection produces end-organ disease that mimics that associated with vertically transmitted CMV infection in humans (Bantug et al. 2008; Li et al. 2008). Furthermore, employment of transgenic mice enables the identification of genes critical to CMV infection and the immune response associated with viral infection.

Studies of viral brain infection in adult and neonatal mice suggest that host immune activation contributes to viral-associated neurological damage (Armien et al. 2009;

Cheeran et al. 2009b; Marques et al. 2008). Indeed, the progression of MCMV brain infection in neonatal mice pivots on innate and adaptive immune responses (Bantug et al. 2008). Recruitment of neutrophils and macrophages is the primary innate defense mechanism against viral infection and is critical in controlling virus proliferation and dissemination (Nesin and Cunningham-Rundles 2000). Macrophages aid in tissue repair, cytokine production, and removal of cytopathic debri, but they can also be harmful to neighboring cells by their overactivation and the production of reactive oxygen species (ROS). Increases in macrophage ROS have been described during acoustic inner ear trauma and contribute to the lethality of spiral ganglion neurons (SGNs) and hair cells in the mammalian cochlea (Hirose et al. 2005). Still, very little is known about the contribution of proinflammatory immune responses to CMV-related SNHL.

In the present study, we describe a model of congenital MCMV infection that resulted in viral infection of the mouse inner ear as well as bilateral hearing loss. Active MCMV was detected in cochlear SGNs and perilymphatic epithelial cells but was absent from the organ of Corti, including the inner and outer hair cells. Interestingly, most hair cells were eliminated by 21 dpi despite a lack of direct viral infection. Furthermore, we showed a robust innate immune response during cochlear MCMV infection that persisted long after viral clearance. Taken together, these data suggest an important role for inflammation during MCMV-induced SNHL, including the indirect death of cochlear hair cells.

Methods

Virus and animals

RM461, a recombinant cytomegalovirus expressing *Escherichia coli* β-galactosidase under the control of the human ie1/ie2 promoter/enhancer (Stoddart et al. 1994), was kindly provided by Edward S. Mocarski. MCMV-GFP, a recombinant MCMV strain (K181 MC.55 [$ie2^{-}$ GFP^{+}]) (van Den Pol et al. 1999) that expresses the reporter green fluorescent protein, was kindly provided by Jon D. Reuter. In this virus, GFP is inserted into the MCMV ie2 locus and driven by the human elongation factor-1a promoter, resulting in GFP expression during active viral replication. Each virus was maintained by passage in weanling female BALB/c mice. Salivary gland-passed virus was then grown in NIH 3T3 cells for two passages, which minimized any carryover of salivary gland tissue. Infected 3T3 cultures were harvested at 80% to 100% cytopathic effect and subjected to three freeze–thaw cycles. Cellular debris was removed by centrifugation (1,000×*g*) at 4°C, and the virus was pelleted through a 35% sucrose cushion (in Tris-buffered saline [50 mM Tris–HCl, 150 mM NaCl, pH 7.4]) at 23,000×*g* for 2 h at 4°C. The pellet was resuspended in Tris-buffered saline containing 10% fetal bovine serum (FBS). Viral stock titers were determined on 3T3 cells as 50% tissue culture infective doses ($TCID_{50}$) per milliliter. Virulent, salivary gland-passaged, sucrose gradient-purified virus was used for all intracerebral infections. SNHL measurements, flow cytometry, inflammatory cell immunohistochemistry, and quantitative PCR were performed with RM461 virus while immunohistochemical detection of MCMV during viral infection was performed with the MCMV-GFP virus.

Virus inoculation

Neonatal mice (1 day old) were placed on ice for 3 min to induce anesthesia before being secured in a cooled stereotaxic apparatus (Stoelting Co., Wood Dale, IL), equipped with a Cunningham mouse adapter modified to fit neonatal mice. The stereotaxic apparatus was maintained at 4°C to 8°C by a dry ice/ethanol reservoir. A 10 μL syringe with a cemented 1.7-in. 26-G needle (Hamilton Company) was used to inject MCMV (RM461 or MCMV-GFP) into the right lateral cerebral lobe as previously described (Mutnal 2011). MCMV was diluted in saline and injected at 500 $TCID_{50}$ in a volume <3 μl. Saline was used for control intracerebral injections. Animal experiments were performed in accordance with a protocol approved by the Institutional Animal Care and Use Committee at the University of Minnesota, NINDS, NIDA, and the NIH.

Auditory-evoked brainstem response

Hearing loss was quantified at ages >P21 by measuring the auditory brainstem response (ABR). Uninjected, saline-injected, or MCMV-infected mice were placed under anesthesia using a combination of Ketamine and Xylazine (100 mg and 10 mg/Kg body weight, respectively). Needle electrodes were placed subcutaneously with the positive electrode placed on the vermis of the nose, the reference electrode under the pinna of the stimulated ear and the ground on the contralateral dorsal abdomen. Stimuli were presented as broadband clicks and responses to 1,000 sweeps were averaged at each intensity level using 10-dB sound pressure level (SPL) steps. Auditory threshold was determined as the lowest intensity level at which a clear waveform was visible in the evoked trace by visual inspection. An ABR value of 90 dB SPL was assigned to cochleae that failed to stimulate an ABR waveform at 80 dB SPL, the highest stimuli presented in this study, although this value may greatly underestimate the increased

thresholds in these animals. Auditory stimuli were generated using SigGenRP software and evoked potentials were collected and analyzed with BioSigRP TDT System 3 (Tucker-Davis Technology; Alachua, FL). Calibration was achieved via SigCalRP and applied to a normalization file in SigGenRP.

Immunohistochemistry

Preparation of the cochleae for immunohistochemistry was based on a modified protocol of Whitlon et al. (Alam et al. 2007; Whitlon et al. 2001). Mice were exsanguinated at 7, 14, and 21 dpi by transcardial perfusion with 0.1 M phosphate-buffered saline (PBS), pH 7.4, containing 0.1% sodium nitrite, then with 20 mL of 4% paraformaldehyde in phosphate buffer (PB) at room temperature (RT). The mice were then decapitated, the cochleae exposed, and an additional 1.0 mL of fixative was lightly perfused through the round and oval window. The excised cochleae were immersed in fixative (4% paraformaldehyde in 0.1 M PB) overnight at 4ºC, washed with PBS, and decalcified by immersion in 0.12 M EDTA, pH 7.0 for 1 week at RT. The decalcified cochleae were infiltrated with sucrose and then embedded in Tissue-Tek® O.C.T™ Compound. Serial 20 μm thick mid-modiolar sections were cut on a freezing microtome and mounted on poly-L-lysine-coated glass slides. Slides were stored at −20°C until further use. The slides were dried at RT for 10 min, washed in PBS, permeabilized with 0.4% Triton X-100 in PBS for 20 min at RT, washed in PBS, and transferred to blocking buffer (PBS containing 5% goat serum and 2% bovine serum albumin) for 1 h at RT, prior to application of primary antibodies.

Primary antibodies of rabbit anti-myosin VIA (Sigma–Aldrich, St. Louis, MO) and mouse anti-NF200 (Sigma–Aldrich, St. Louis, MO) were used as markers for inner and outer cells and spiral ganglion neurons, respectively. Rat anti-CD11b (BD PharMingen, San Diego, CA) and rat anti-CD3 (BD PharMingen, San Diego, CA) were used to label brain infiltrating immune cells. All antibodies were incubated in blocking buffer. Following overnight incubation of the sections in primary antibodies at 4°C, the sections were rinsed in PBS and secondary antibodies applied for 1 h at RT. Secondary antibodies used were donkey anti-mouse and -rabbit Rhodamine red (Jackson Laboratories) as well as goat anti-rat 594 (Invitrogen, Carlsbad, CA). Sections were counterstained with Hoechst 33342 (1 μg/ml; Chemicon, Temecula, CA) in PBS for 20 min at RT in the dark.

Quantitative real-time PCR

Six cochleae, taken from three mice, were pooled for each experiment and homogenized in TRIzol (Invitrogen, Carlsbad, CA) using a polytron tissue homogenizer. cDNA was synthesized with 0.5 to 1.0 μg of total RNA from uninfected and MCMV-infected mouse cochleae at 7, 14, and 21 dpi, using Superscript II reverse transcriptase (Invitrogen, Carlsbad, CA) and oligo dT6–12 primers (Sigma–Genosys, The Woodlands, TX). PCR was performed with the Advantage SYBR Green QPCR master mix (Stratagene, La Jolla, CA). The PCR conditions for the Mx3000P QPCR System (Stratagene) were: 40 denaturation cycles of 95°C for 10 s, annealing at 60°C for 10 s, and elongation at 72°C for 10 s. The relative product levels were quantified using the 2(−Delta Delta C(T)) method (Livak and Schmittgen 2001) and were normalized to the housekeeping gene hypoxanthine phosphoribosyl transferase-encoding (HPRT; NM_013556). Data presented are representative of three independent experiments. Forward and reverse primer sequences used in the study: inducible nitric oxide synthase (iNOS; NM_010927): 5′-tggccacctgttcagc tacg-3′ and 5′-gccaaggccaaacacagcata-3′; tumor necrosis factor-α (TNFα; NM_013693): 5′-ctgtgaagggaatgggtgtt-3′ and 5′-ggtcactgtcccagcatctt-3′; interleukin-6 (IL-6; NM_031168): 5′-caagccagagtccttcagag-3′ and 5′-gagcattg-gaaattggggta-3′; interferon γ (IFNγ; NM_008337): 5′-gcgtcattgaatcacacctg-3 and 5′-gacctgtgggttgttgacct-3′; interleukin-10 (IL-10; NM_010548): 5′-ccctttgctatggtgtcctttt-3′ and 5′-tggtttctcttcccaagacc-3′; heme oxygenase-1 (HO-1; NM_010442): 5′-cacgcatatacccgctacct-3′ and 5′-cca gagtgtt cattcgagca-3′; glutathione peroxidase-1 (Gpx1; NM_008160): 5′-gtccaccgtgtatgccttct-3′ and 5′-cctcaga gagacgcgacatt-3′; MCMV glycoprotein B (gB): 5′-cgctggtcgtctttcagttc-3′ and 5′-ctgttcgtgtcgcagttctc-3′.

Flow cytometric leukocyte and reactive oxygen species detection

Cochlear tissues from three animals (6 cochleae) were harvested, pooled in ice-cold HBSS, and digested in TrypLE™ Select (Invitrogen, Carlsbad, CA) for 30 min at 37°C. Cochlea were applied directly to a 40-μm filter atop a 50-mL conical and mashed through the filter with the blunt end of a syringe plunger. To retrieve all cells and deactivate the digestion cocktail, the filter was rinsed multiple times with HBSS containing Mg^{2+}/Ca^{2+}. Cochlear cells were centrifuged at 600×*g* for 5 min and resuspended in Fc Block (anti-CD32/CD16 in the form of 2.4 G2 hybridoma culture supernatant with 2% normal rat and 2% normal mouse serum) to inhibit nonspecific antibody binding. Cochlear leukocytes were stained with anti-mouse immune cell surface markers for 45 min at 4°C (anti-CD45-allophycocyanin (eBioscience), anti-CD11b-allophycocyanin-CY7, anti-Ly6G-PE (BD Biosciences)) and analyzed by flow cytometry. Following cell surface marker staining, cells were loaded for 30 min at 37°C with the intracellular reactive oxygen species indicator, 2′,7′-

dichlorodihydrofluorescein diacetate (DCFH-DA; 20 μM; St. Louis, MO), rinsed, and resuspended in 1 mL PBS with 2% FBS for flow cytometry. Live leukocytes were gated using forward scatter and side scatter parameters on a BD FACSCanto flow cytometer (BD Biosciences). Control isotype antibodies were used for all isotype and fluorochrome combinations to assess nonspecific antibody binding. Data was analyzed using FlowJo software (TreeStar).

Statistical analysis Student's *t* test paired assuming unequal variance (Microsoft Excel) was used to compare ABR and quantitative PCR data.

Results

Intracerebral delivery of MCMV to neonatal mice resulted in hearing loss

Neonatal Balb/c mice were injected into the right cerebral lobe with either saline or the RM461 strain of MCMV (500 $TCID_{50}$) no later than 24 h after birth. Previous studies from our laboratory have shown that neonatal injection of MCMV into the right cerebral lobe establishes a robust central nervous system infection (Mutnal 2011), confirming viral delivery into the brain. As the infection progressed, phenotypic signs of MCMV infection were also noted such as: weight loss, brain microcephaly, and ventricular calcifications. Control uninjected and saline-injected mice developed normally.

At 3 weeks post-infection (i.e., 3 weeks postnatal), the age where mouse auditory thresholds are considered mature (Song et al. 2006), both control and MCMV-infected mice were tested for the presence of an ABR. As a gauge of general auditory capacity, a series of broadband clicks were presented in decreasing intensity (80 dB SPL to 0 dB in −10-dB increments) to each ear separately. In uninfected control and saline-injected mice, ABRs were detectable down to the 40 dB SPL sound intensity level. In contrast, presentation of an 80 dB SPL stimulus, the highest presented intensity, was unable to evoke an ABR in the majority of neonatal mice infected with MCMV. Figure 1 shows a dot plot, including the mean and standard deviation, of ABR thresholds for individual ears in control, saline, and MCMV-injected mice. While 100% of MCMV-infected mice exhibited hearing loss, five out of 13 MCMV-infected mice had asymmetric SNHL with ABR thresholds differing between the two ears. Table 1 presents ABR threshold data for individual CMV-infected mice. Left and right ears are listed separately to illustrate SNHL asymmetry.

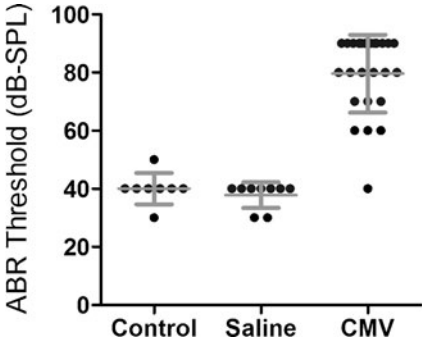

Fig. 1 Intracerebral delivery of MCMV to neonatal mice results in profound sensorineural hearing loss. Dot plot of ABR thresholds for individual ears in uninjected control (n=4 mice; eight cochlea), saline-injected (n=5 mice; nine cochlea) and MCMV-injected mice (n=13 mice; 24 cochlea) at 21 dpi. Mean ABR and standard deviation are represented in *gray*. The mean ABR threshold in saline-injected mice did not differ from uninjected control mice (p=0.369). MCMV-injected mice exhibited ABR thresholds of ~80 dB SPL which was significantly increased compared to both control and saline-injected mice (p<0.001). ABR click stimuli were presented from 80 dB SPL to 0 dB in descending −10-dB increments, and responses to 1,000 sweeps were averaged at each intensity level

Hair cell loss was associated with hearing loss during MCMV cochlear infection

To investigate the pathology of hearing loss, MCMV-infected and saline-injected mice were perfused at 7, 14, and 21 dpi. Cochleae were extracted, cryosectioned, and assessed for the presence or absence of inner and outer hair cells (Fig. 2a–f). Using myosin VIA as a marker for hair cells, we found that the organ of Corti cytoarchitecture was

Table 1 ABR threshold data for MCMV-infected mice at 21 dpi

Animal	ABR threshold (dB-SPL)	
	Right	Left
CMV 1	>80	80
CMV 2	>80	>80
CMV 3	>80	>80
CMV 4	60	80
CMV 5	60	>80
CMV 6	60	40
CMV 7	>80	80
CMV 8	70	70
CMV 9	70	-
CMV 10	80	80
CMV 11	>80	>80
CMV 12	>80	>80
CMV 13	>80	80
Mice with SNHL	100%	
Mice with asymmetric SNHL	46%	

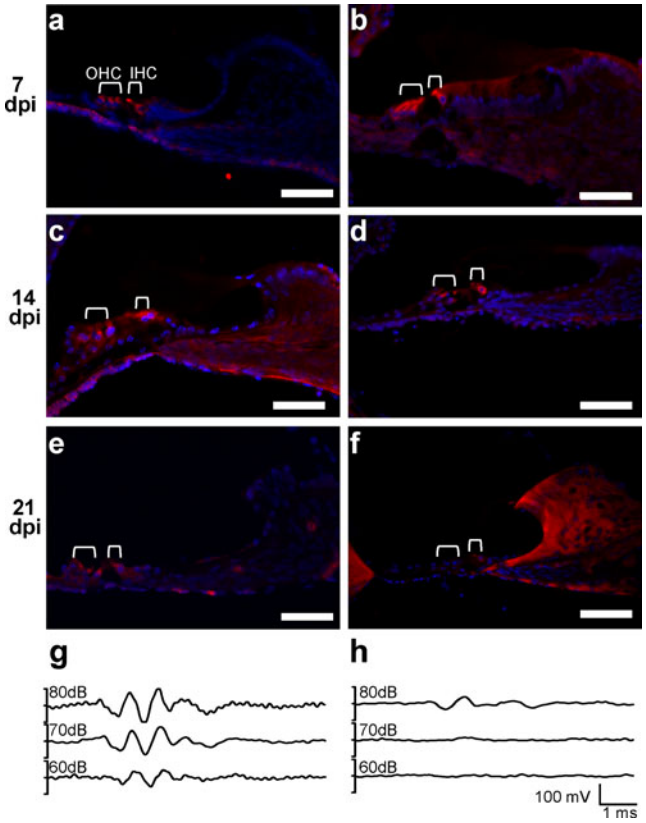

Fig. 2 MCMV-induced SNHL correlates with the progressive loss of inner and outer cochlear hair cells. Immunohistochemical staining for myosin VIA (*red*), a marker for cochlear hair cells, and the nuclear counterstain Hoechst 33342 (*blue*) was performed on mid-modiolar cochlear sections at 7 (**a**, **b**), 14 (**c**, **d**), and 21 dpi (**e**, **f**). One inner and three outer hair cells are visible at all ages in the saline-injected mice (**a**, **c**, **e**) and at 7 (**b**) and 14 dpi (**d**) in MCMV-infected mice. Most hair cells are gone by 21 dpi in MCMV-infected mice. **f** Isolated inner hair cells were detected at 21 dpi in MCMV-injected mice. For cochlea shown in **e** (saline) and **f** (MCMV), ABR measurements were taken prior to cochlear dissection and are represented in **g** (saline) and **h** (MCMV). Note that the MCMV-infected cochlea retaining inner hair cells at 21 dpi (**f**) shows a diminished ABR threshold (**h**) compared to saline-infected mice. *Image scale bar*=50 μm

largely preserved at 7 dpi (Fig. 2a, b) and 14 dpi (Fig. 2c, d). In sharp contrast, myosin VIA staining at 21 dpi revealed loss of both inner and outer hair cells in cochleae taken from MCMV-infected mice indicating that the bulk of inner and outer hair cell death during MCMV infection occurred between 14 and 21 dpi. In agreement with asymmetric hearing loss (Fig. 1), MCMV-infected mice with residual hearing at 21 dpi (Fig. 2h) retained isolated hair cells in the organ of Corti at 21 dpi (Fig. 2f). In contrast, robust myosin VIA staining was observed in 21 dpi saline-infected mice with normal ABR thresholds (Fig. 2e, g). In MCMV-infected mice with remaining ABRs and hair cells, inner hair cells were largely the only sensory cell preserved suggesting a higher susceptibility of outer hair cells to MCMV infection.

SGNs and perilymphatic epithelial cells, but not hair cells, were sites of viral infection

We next investigated whether MCMV-induced hair cell loss was due to direct MCMV infection of these cells or was indirectly related (i.e., bystander) to the primary infection. To this end, we first determined the kinetics of a productive MCMV cochlear infection via qPCR detection of the late MCMV gene product, gB. qPCR analysis of gB mRNA expression indicated that viral infection of the cochlea peaked at 7 dpi and dropped below the threshold of detection by 14 dpi (Fig. 3a). These data corroborate previously published kinetics of cochlear MCMV infection (Kosugi et al. 2002) and indicate that viral infection was cleared prior to hair cell loss (between 14 and 21 dpi).

Next, for histochemical detection of MCMV infection, we intracranially injected neonates with a recombinant MCMV that expresses GFP (MCMV-GFP). The extent and percentage of mice exhibiting SNHL in neonatal mice infected with MCMV-GFP equaled that in neonates infected with the RM461 viral strain (data not shown). At 7 dpi, mid-modiolar cochlear sections confirmed robust MCMV infection in the cochlea (Fig. 3b). MCMV positive cells were preferentially detected in perilymphatic compartments including the scala tympani and scala vestibuli (Fig. 3c). Endolymphatic compartments were void of virus at 7 dpi. Immunohistochemical studies showed partial colocalization of MCMV-GFP with NF200, a SGN intermediate filament (Fig. 3d). Interestingly, MCMV-GFP did not colocalize with myosin VIA and the organ of Corti was completely void of MCMV-GFP positive cells at 7 dpi (Fig. 3e). The cochlea was absent of MCMV-GFP at 14 and 21 dpi corroborating the time course of gB qPCR detection in MCMV-infected cochleae.

Neonatal MCMV infection induced robust and persistent innate immune responses in the cochlea

To investigate the kinetics of cochlear immune cell infiltration during neonatal MCMV infection, cochlear single cell suspensions were immunostained with markers characteristic of macrophage populations (i.e., CD45 and CD11b). Using these markers, flow cytometry identified two distinct populations of cells in the MCMV-infected cochlea: CD45 (+) CD11b $(+)^{high}$ cells, which represented infiltrating macrophages, and $CD45^{high}CD11b^{-}$, largely composed of $CD3^{+}$ lymphocytes. Neonatal mice infected with 500 $TCID_{50}$ MCMV (RM461) had increased macrophage (4.24%) infiltration at 7 dpi compared to control (0.64%; Fig. 4a). An elevated percentage of CD45 (+) CD11b $(+)^{high}$ cells was maintained at 14 dpi (3.83%; Fig. 4b). Confirmatory antibody staining for CD11b revealed abundant CD11b (+) cells at 7 dpi with fewer

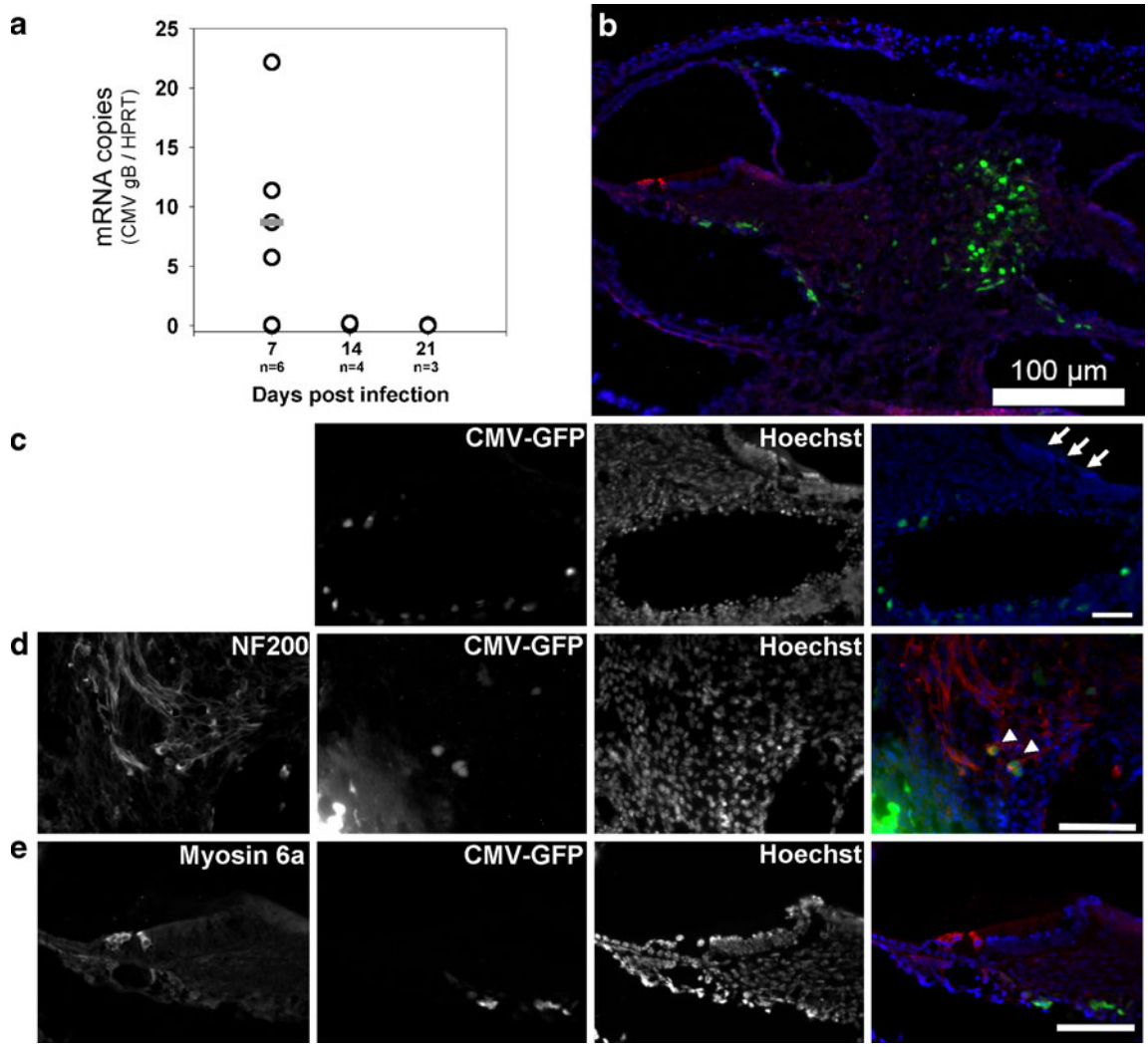

Fig. 3 Spiral ganglion neurons and perilymphatic epithelial cells, but not inner or outer hair cells, support MCMV infection. **a** Quantitative RT-PCR for MCMV glycoprotein B mRNA detected active MCMV infection at 7 dpi with no gB mRNA detection at either 14 or 21 dpi. For each sample, MCMV gB mRNA copy number was normalized to the housekeeping gene, HPRT. MCMV colocalization studies were performed on mid-modiolar cochlear sections from 7 dpi mice (**b**–**e**). **b** Low magnification view of the cochlea showing MCMV-GFP-infected cells (*green*), myosin VIA (*red*), and Hoechst 33342 (*blue*). **c** Cross section through the organ of Corti showing MCMV-GFP-positive cells (*green*) around the perilymphatic compartment. *Arrows* indicate the location of the organ of Corti. **d** MCMV-GFP-infected cells (*green*) colocalize with NF200 (*red*), a marker of SGNs. *Arrowheads* indicate GFP and NF200 double positive cells. **e** MCMV-GFP-positive cells (*green*) in the epithelium surrounding the perilymphatic compartment. Again, myosin VIA-labeled hair cells are void of MCMV-GFP (*green*). **c**–**e** are counterstained with Hoechst 33342 (*blue*). *Scale bar* in **c**–**e** is 50 µm

cells at 14 dpi in MCMV-infected but not saline-infected (Fig.5a–d). Consistent with the surface expression of CD11b, the immunofluorescence of CD11b (+) cells in the cochlea of MCMV-infected mice revealed a membranous pattern surrounding clearly Hoechst-stained nuclei. Cochlear infiltrating macrophages, at 7 dpi, were found at with sites of active MCMV infection (Fig. 5b).

Macrophage production of ROS is an effective method for combating primary infection. ROS production, while beneficial in clearing invading pathogens, can also cause irreparable harm via bystander damage to surrounding cells. Using 2′,7′-DCFH-DA, a fluorescent indicator of intracellular ROS, we quantified macrophage ROS production during MCMV infection. In MCMV-infected cochlea, 74.4% of infiltrating macrophages produced high levels of ROS at 7 dpi (Fig. 4a) and continued to produce ROS at 14 dpi (53.8%; Fig. 4b). ROS production in saline-injected mice was not quantifiable due to low numbers of macrophage infiltrates at 7 and 14 dpi.

Flow cytometry also identified a population of $CD45^{high}CD11b^{-}$ cells during the course of cochlear MCMV infection. The number of $CD45^{high}CD11b^{-}$ cells

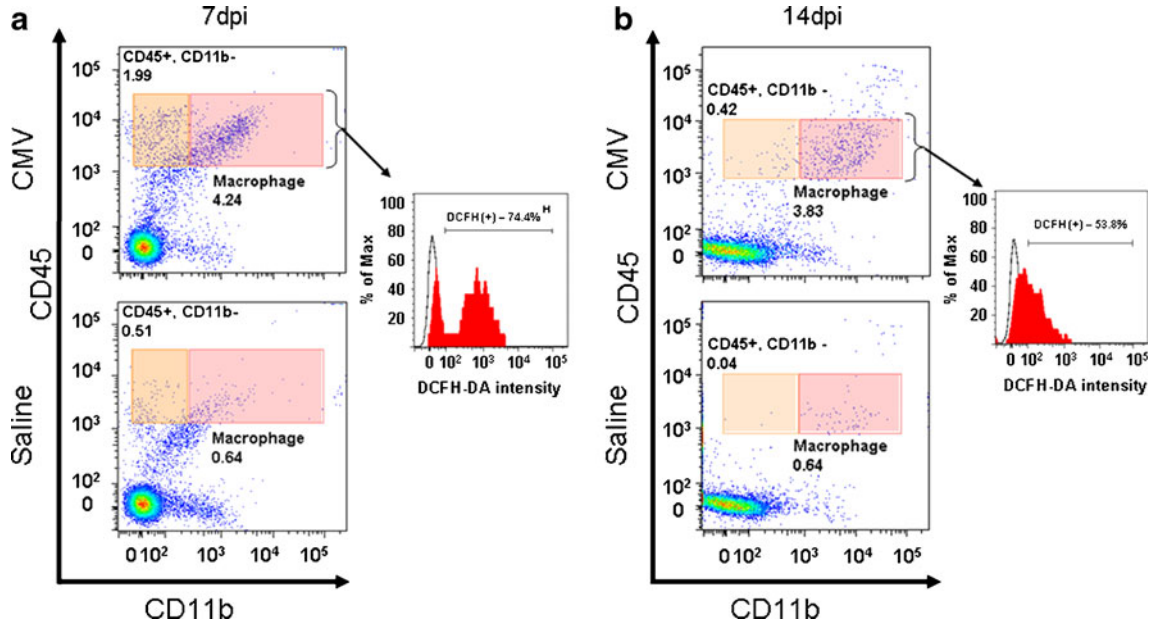

Fig. 4 Cochlear MCMV infection induces robust and persistent peripheral immune cell infiltration. Cochlear-infiltrating leukocytes were isolated from MCMV- or saline-injected mice at 7 (**a**) and 14 dpi (**b**). Cell populations were identified using fluorescent-conjugated antibodies, CD11b-APC and CD45-APC-Cy7, and analyzed with flow cytometry. CD45 (+) CD11b $(+)^{high}$ macrophages from MCMV-infected mice were analyzed at 7 and 14 dpi for DCFH-DA reactivity, an indicator of intracellular ROS. DCFH-DA gates for MCMV-infected mice (*red*) were drawn based on unloaded cells from the same brain cell preparation (*black line*). Macrophage ROS levels are increased at 7 dpi (**a**) and persist through 14 dpi (**b**). ROS was not quantifiable in saline-injected mice due to the lack of infiltrating macrophages in the absence of infection

was elevated above saline-injected controls at both 7 dpi (MCMV=1.99% v. saline=0.51%) and 14 dpi (MCMV=0.42% v. saline=0.04%; Fig. 4a, b). Antibody staining for CD3 in MCMV-infected cochlear cryosections confirmed the kinetics of $CD45^{high}CD11b^{-}$ infiltrate identified using flow cytometry (Fig. 5e–i). As with CD11b, CD3 is also a surface protein. In our preparations, immunofluorescence of CD3-positive cells in the cochlea of MCMV-infected mice revealed a membranous pattern surrounding nuclei clearly stained with Hoechst. These data show robust and persistent immune infiltration in the neonatal cochlea following MCMV infection.

Proinflammatory mediators are increased during neonatal CMV infection

During infection, proinflammatory cytokines and chemokine production is concomitant with immune cell invasion. Therefore, mRNA expression levels of proinflammatory mediators were examined at 7, 14, and >21 dpi (Fig. 6) in both MCMV-infected and saline-injected mice using qRT-PCR. All proinflammatory mediator expression levels were normalized to their respective saline-injected controls at each time point. Intracranial MCMV injection dramatically increased TNFα and IL-6 gene expression at 7 dpi. While mRNA levels of TNFα and IL-6 decreased throughout the course of the infection, their expression remained elevated out to 21 dpi. Similarly, IFNγ showed increased gene expression at 7 dpi with levels tapering down, but still elevated, by 21 dpi. iNOS, a proinflammatory molecule, also increased at 7 dpi in MCMV-infected cochlea. Peak iNOS expression at 14 dpi was drastically reduced at 21 dpi, although still elevated compared to control cochlea. Interestingly, the anti-inflammatory cytokine, interleukin-10 (IL-10), was upregulated during the peak of infection, suggesting a mechanism to mitigate the proinflammatory response.

Viral infection induced weak antioxidant responses

Excessive and prolonged ROS has been implicated in neurotoxicity during viral brain infection (Schachtele et al. 2010). Cellular neutralization of ROS is dependent on the expression of antioxidant genes, such as Gpx1 and heme oxygenase-1 (HO-1). Using quantitative RT-PCR, we investigated the gene expression profile (7, 14, and 21 dpi) of both Gpx1 and HO-1 during neonatal MCMV infection (Fig. 7). Expression of HO-1 was increased at 14 dpi, but not at 7 or 21 dpi. MCMV infection did not significantly increase Gpx1 gene expression over saline controls at 7, 14, or 21 dpi. These data indicate a weak antioxidant stress response to combat excessive ROS production in the cochlea during MCMV infection.

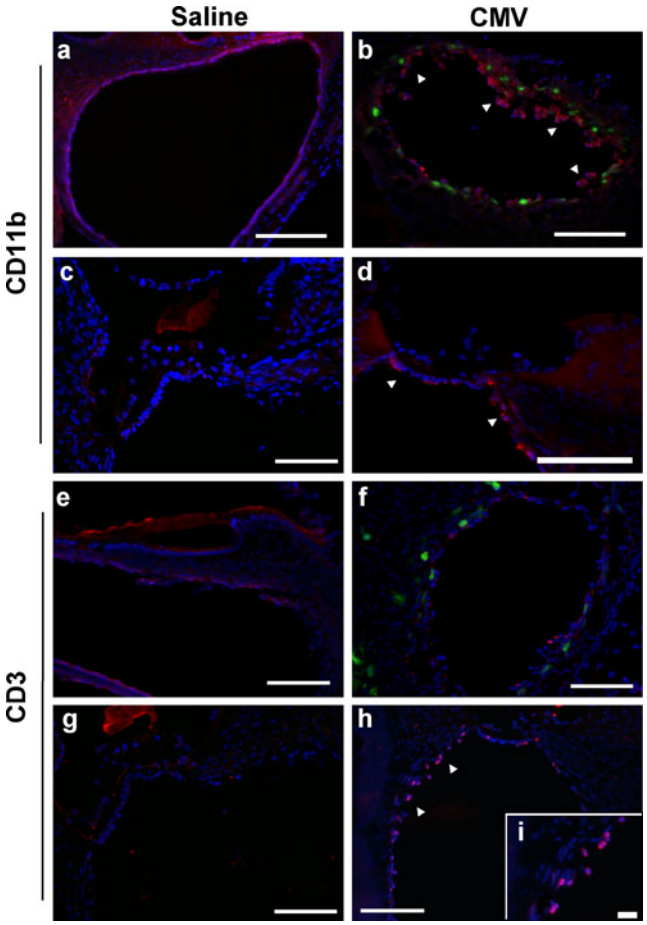

Fig. 5 CD11b+ and CD3+ cells infiltrate the cochlea during MCMV infection at 7 and 14 dpi. Saline-injected and MCMV-infected neonatal mice were fixed and cochleae removed at 7 (**a**, **b**, **e**, **f**) and 14 dpi (**c**, **d**, **g**, **h**). **a**–**d** *Arrowheads* highlight regions containing CD11b-positive immune cells. Immunohistochemical staining for CD11b (*red*) at 7 dpi shows that macrophages populate cochlear regions also positive for MCMV-GFP (**b**). CD11b cells remain in cochlea at 14 dpi (**d**). No CD11b positive cells were detected in saline-injected mice at 7 (**a**) or 14 dpi (**c**). **e**–**h** *Arrowheads* highlight regions containing CD3 positive immune cells. MCMV-infected cochlear tissue stains positive for CD3+ T-cells (*red*) at 7 (**f**) and 14 dpi (**h**), but not in saline infected mice (**e**, **g**). **i** Higher magnification view of CD3 + T-cells at 14 dpi. Images **a**–**i** are counterstained with Hoechst 33342 (*blue*). *Scale bar* in **a**–**h** is 50 μm; *scale* in (**i**) is 20 μm

Discussion

Congenital CMV infection is the leading cause of SNHL in children, contributing to approximately 14–25% of all congenital hearing loss cases (Cheeran et al. 2009a). In this study, a neonatal mouse model of profound SNHL via intracerebral infection of MCMV is described. Using this model, MCMV infection induced cochlear hair cell death by 21 dpi, despite a lack of direct MCMV infection of hair cells and the complete clearance of the virus from the cochlea by 14 dpi. Our data show that MCMV-induced hearing loss and hair cell death is associated with a prolonged cochlear inflammatory infiltrate and high levels of macrophage-produced ROS.

In this study, direct inoculation of the brain with MCMV resulted in SNHL and viral labyrinthitis in 100% of the infected mice. Immunohistochemical analysis at 7 dpi found that in the cochlea, MCMV directly infected epithelial cells of the perilymphatic compartments, including the scala tympani and scala vestibuli and SGNs (Fig. 3). In contrast, cells in the organ of Corti, including the inner and outer hair cells, were not infected. These findings resonate along with immunopathology reported in CMV-infected humans as well as guinea pig and mouse models of CMV infection (Grosse et al. 2008; Park et al. 2010).

The pattern of MCMV-GFP-positive cells in the cochlea at 7 dpi is consistent with viral expansion through the internal auditory canal, connecting the ventricular cerebral spinal fluid with the cochlear perilymphatic compartments, or meningogenic viral entry (Davis and Hawrisiak 1977). Indeed, the ventricular reservoirs of the brain are contiguous with the cochlear perilymphatic compartments and have been reported as a route of CMV viral entry into the inner ear (Li et al. 2008; Otis and Brent 1954). Infectious agents can also enter the cochlea via typanogenic (through the round window) and hematogenic (through the blood) routes. Previous studies have shown that peripheral (intraperitoneal) inoculation with MCMV can also result in central nervous system and cochlear infection (Bantug 2008; Cekinovic 2008; Li 2008). While intracranial viral delivery, as used in this study, induces a robust CNS viral infection, and the viral pathology is consistent with meningogenic viral entry, we cannot completely discount the possibility that virus dissemination into the cochlea is a result of a peripheral infection secondary to the CNS infection.

In the majority of MCMV-injected mice, cochlear infection resulted in profound hearing loss as measured by the inability to evoke a prototypical ABR waveform with high intensity click stimuli (Fig. 1). The prototypical ABR consists of five waveforms. Systematic ablation studies in rats attributes the generation of wave form 1 in the ABR profile to evoked potentials in the auditory nerve while wave forms 2 through 5 are associated with activity in higher central nuclei (Caird and Klinke 1987; Chen and Chen 1991; Funai and Funasaka 1983). In the present study, the lack of ABR wave 1 in MCMV-infected mice indicates that the histochemically detected loss of hair cells significantly contributes to viral-induced hearing loss. However, intracranial MCMV infection also results in a robust central nervous infection making it difficult to fully attribute MCMV-related hearing loss to peripheral hair cell death.

Greater than 20% of asymptomatic congenitally infected infants with human CMV-induced SNHL exhibit asymmet-

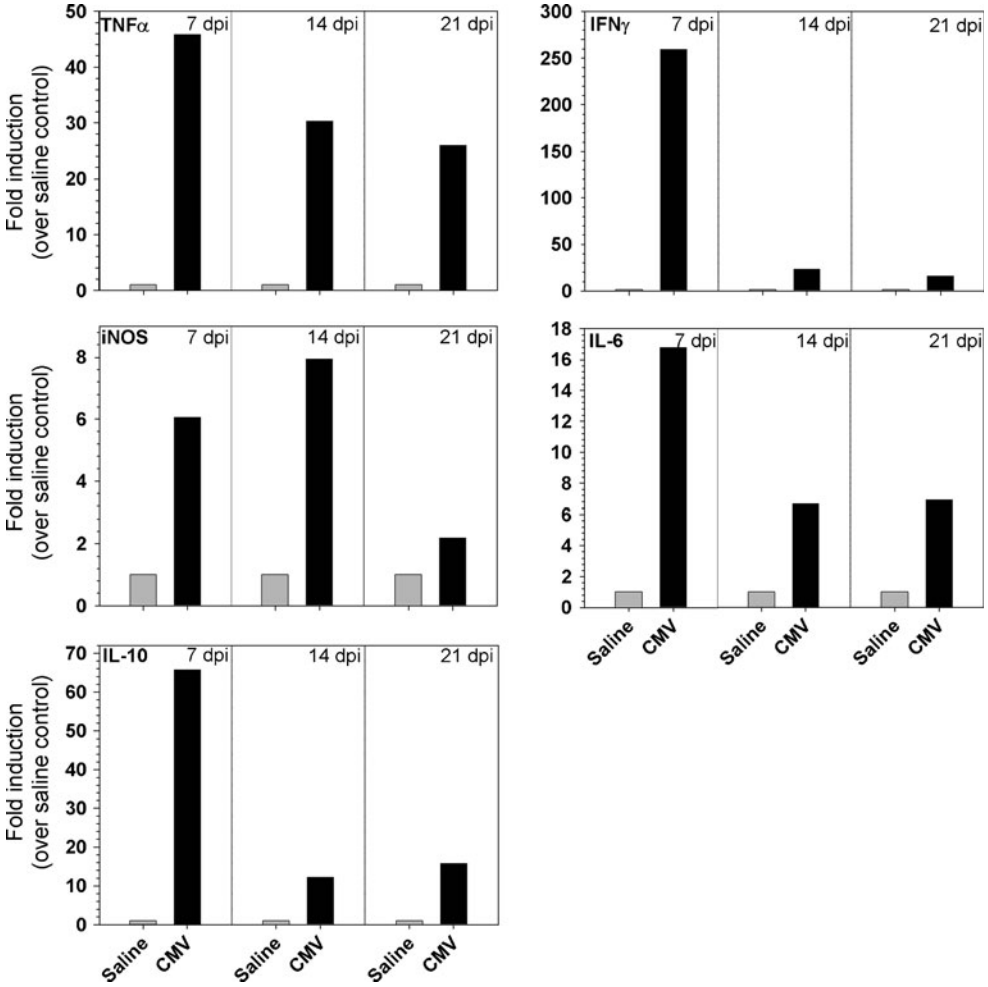

Fig. 6 Robust and persistent induction of proinflammatory gene expression in the cochleae during neonatal MCMV infection. Cochleae were isolated and RNA extracted from saline-injected and MCMV-infected neonates at 7, 14, and 21 dpi. Quantitative RT-PCR was performed, and mRNA levels were normalized to the housekeeping gene, HPRT. Data are presented as the fold induction over saline controls. Quantitative PCR was performed on the proinflammatory mediators TNFα, IFNγ, iNOS, and IL-6, as well as the anti-inflammatory cytokine IL-10. Cochleae from three mice were pooled for each condition at every time point. The data presented are representative of three separate experiments

ric hearing loss (Fowler et al. 1997). Similarly, MCMV-induced hearing loss was asymmetric as evidenced by intra-animal ABR variation between ears. These data were confirmed by the detection of residual hair cells in the cochleae which have retained a degree of hearing at 21 dpi (Fig. 2). The observed asymmetrical hearing loss may be attributable to the unequal meningogenic viral dissemination from the CNS to the inner ear as well as an asymmetric cochlear immune response, which has been reported during models of otitis media (Matkovic et al. 2007).

Our data indicate that MCMV-induced hearing loss is not due to direct viral infection of hair cells but rather is associated with extensive labyrinthitis initiated in response to infection. Not only were hair cells void of MCMV infection, but quantitative RT-PCR for MCMV gB mRNA indicated that active viral infection was cleared by 14 dpi (Fig. 3). gB is expressed during the late phase of the viral replication cycle and qPCR for gB mRNA may not account for all infected cells at 14 and 21 dpi. However, histological analysis of cochleae corroborates these gene expression studies by confirming the absence of MCMV-GFP at 14 and 21 dpi (data not shown). In all cases examined, MCMV-GFP was absent from the inner and outer hair cells as well as the supporting cells of the organ of Corti at 7 dpi, suggesting secondary mechanisms of pathogenesis.

Previous studies of MCMV brain infection in mice indicate the immune response as pivotal to control viral dissemination and promote clearance (Bantug et al. 2008; Cheeran et al. 2001, 2004, 2009b). However, it is becoming increasingly clear that although an immune response is important in the clearance of invading pathogens, exaggerated or sustained inflammation can be detrimental to healthy cells in the tissue surrounding the infection (Marques et al. 2008). Colocalization studies for MCMV-GFP and myosin VIA clearly show the loss of hair cells, despite the inability of MCMV to directly infect these cells. Hair cell loss occurred between 14 and 21 dpi, correlating with persistent detection of macrophage and T-cell populations (Fig. 4), prolonged proinflammatory mediator production (Fig. 5), as well as the absence of MCMV gB mRNA detection (Fig. 3).

Cochlear hair cells are known to be preferentially sensitive to inflammation and oxidative damage (Choung et al. 2009; Henderson et al. 2006; Kim et al. 2010). In

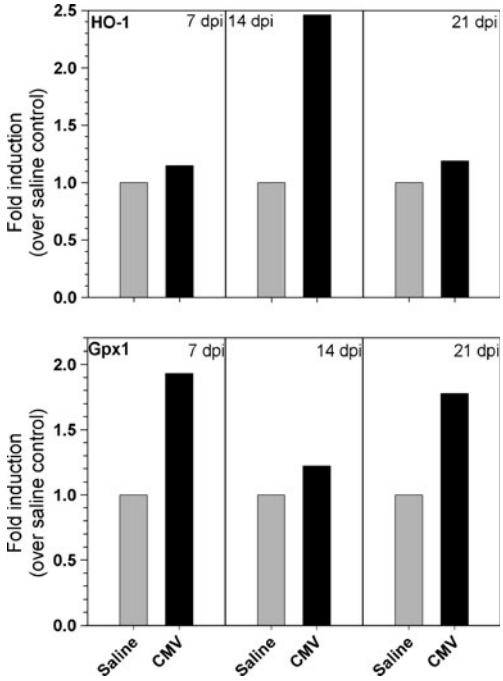

Fig. 7 Weak antioxidant response during cochlear MCMV infection. Cochleae were isolated and RNA extracted from saline-injected and MCMV-infected neonates at 7, 14, and 21 dpi. Cochlea from three mice were pooled for each condition at every time point. Quantitative RT-PCR for the antioxidant enzymes Gpx1 and HO-1 was performed and data are presented as the fold induction over saline controls. The data presented are representative of three separate experiments

addition to robust and prolonged induction of proinflammatory cytokines, such as TNFα and IL-6 (Fig. 5), we observed persistent increases in cochlear ROS (Fig. 4). TNFα and IL-6, released by cochlear spiral ligament fibrocytes during bacterial meningitis and autoimmune SNHL (Ichimiya et al. 2000; Van Wijk et al. 2006; Aminpour et al. 2005), can initiate programmed cell death in auditory hair cells (Micheau and Tschopp 2003; Muppidi et al. 2004; Zine and van de Water 2004). Furthermore, macrophage production of ROS contributes to lethal oxidative damage (Ohinata et al. 2000, 2003) of hair cells and SGNs during antibiotic, noise, or age-induced SNHL (Coling et al. 2009; Jeong et al. 2010; Kim et al. 2009; Yamashita et al. 2004). In our model, the MCMV-induced increase in total cochlear ROS levels was due to the sheer quantity of infiltrating macrophages, as well as their persistence following viral clearance, rather than increased free radical production by individual macrophages since the few macrophages detected at 7 dpi in saline-injected mice had similar DCFH-DA levels. Neutralization of ROS via upregulation of intrinsic antioxidants is an effective method utilized by cells to protect from excess free radicals. PCR analysis of antioxidant gene expression revealed a low intrinsic antioxidant response during cochlear MCMV infection, despite high and persistent levels of ROS (Fig. 4).

Proinflammatory cytokine and chemokine production, as well as ROS production, are potential targets for blunting immunopathology associated with cochlear infection. Both TNFα and IL-6 have been targets for anti-inflammatory therapy (Dinh and Van De Water 2009; Ichimiya et al. 2000; Katano et al. 2007; Wakabayashi et al. 2009) , improving hearing in multiple models of cochlear damage (Satoh et al. 2002; Wang et al. 2003; Yamashita et al. 2004). Similarly, strategies to blunt ROS via delivery of antioxidant molecules, like *d*-methionine and *N*-acetylcysteine, have successfully attenuated antibiotic, radiation, and noise-induced hair cell death (Kim et al. 2010; Low et al. 2008). Employment of these strategies may provide a route for hair cell protection in the wake of cochlear MCMV infection.

Acknowledgments We thank Dr. Steven Juhn and Dr. Phil Peterson for their expertise and thoughtful input. This project was supported by Award Number R01 NS-038836 from the National Institute of Neurological Disorders and Stroke, as well as a PharmacoNeuroImmunology training grant (T32DA007097) funded by the National Institute on Drug Abuse. The content is solely the responsibility of the authors and does not necessarily represent the official views of the NINDS, NIDA, or the NIH.

References

Alam SA, Robinson BK, Huang J, Green SH (2007) Prosurvival and proapoptotic intracellular signaling in rat spiral ganglion neurons in vivo after the loss of hair cells. J Comp Neurol 503:832–852

Aminpour S, Tinling SP, Brodie HA (2005) Role of tumor necrosis factor-alpha in sensorineural hearing loss after bacterial meningitis. Otol Neurotol 26:602–609

Armien AG, Hu S, Little MR et al (2009) Chronic cortical and subcortical pathology with associated neurological deficits ensuing experimental herpes encephalitis. Brain Pathol 20 (4):738–750

Bantug GR, Cekinovic D, Bradford R, Koontz T, Jonjic S, Britt WJ (2008) CD8+ T lymphocytes control murine cytomegalovirus replication in the central nervous system of newborn animals. J Immunol 181:2111–2123

Caird DM, Klinke R (1987) The effect of inferior colliculus lesions on auditory evoked potentials. Electroencephalogr Clin Neurophysiol 68:237–240

Cekinovic D, Golemac M, Pugel EP, Tomac J, Cicin-Sain L, Slavuljica I, Bradford R, Misch S, Winkler TH, Mach M, Britt WJ, Jonjic S (2008) Passive immunization reduces murine cytomegalovirus-induced brain pathology in newborn mice. J Virol 82:12172–12180.

Cheeran MC, Hu S, Yager SL, Gekker G, Peterson PK, Lokensgard JR (2001) Cytomegalovirus induces cytokine and chemokine production differentially in microglia and astrocytes: antiviral implications. J Neurovirol 7:135–147

Cheeran MC, Gekker G, Hu S, Min X, Cox D, Lokensgard JR (2004) Intracerebral infection with murine cytomegalovirus induces CXCL10 and is restricted by adoptive transfer of splenocytes. J Neurovirol 10:152–162

Cheeran MC, Lokensgard JR, Schleiss MR (2009a) Neuropathogenesis of congenital cytomegalovirus infection: disease mechanisms and prospects for intervention. Clin Microbiol Rev 22:99–126, Table of Contents

Cheeran MC, Mutnal MB, Hu S, Armien A, Lokensgard JR (2009b) Reduced lymphocyte infiltration during cytomegalovirus brain infection of interleukin-10-deficient mice. J Neurovirol 15:334–342

Chen TJ, Chen SS (1991) Generator study of brainstem auditory evoked potentials by a radiofrequency lesion method in rats. Exp Brain Res 85:537–542

Choung YH, Taura A, Pak K, Choi SJ, Masuda M, Ryan AF (2009) Generation of highly-reactive oxygen species is closely related to hair cell damage in rat organ of Corti treated with gentamicin. Neuroscience 161:214–226

Coling D, Chen S, Chi LH, Jamesdaniel S, Henderson D (2009) Age-related changes in antioxidant enzymes related to hydrogen peroxide metabolism in rat inner ear. Neurosci Lett 464:22–25

Davis GL, Hawrisiak MM (1977) Experimental cytomegalovirus infection and the developing mouse inner ear: in vivo and in vitro studies. Lab Invest 37:20–29

Dinh CT, Van De Water TR (2009) Blocking pro-cell-death signal pathways to conserve hearing. Audiol Neurootol 14:383–392

Fowler KB, McCollister FP, Dahle AJ, Boppana S, Britt WJ, Pass RF (1997) Progressive and fluctuating sensorineural hearing loss in children with asymptomatic congenital cytomegalovirus infection. J Pediatr 130:624–630

Funai H, Funasaka S (1983) Experimental study on the effect of inferior colliculus lesions upon auditory brain stem response. Audiology 22:9–19

Grosse SD, Ross DS, Dollard SC (2008) Congenital cytomegalovirus (CMV) infection as a cause of permanent bilateral hearing loss: a quantitative assessment. J Clin Virol 41:57–62

Henderson D, Bielefeld EC, Harris KC, Hu BH (2006) The role of oxidative stress in noise-induced hearing loss. Ear Hear 27:1–19

Hirose K, Discolo CM, Keasler JR, Ransohoff R (2005) Mononuclear phagocytes migrate into the murine cochlea after acoustic trauma. J Comp Neurol 489:180–194

Ichimiya I, Yoshida K, Hirano T, Suzuki M, Mogi G (2000) Significance of spiral ligament fibrocytes with cochlear inflammation. Int J Pediatr Otorhinolaryngol 56:45–51

Jeong SW, Kim LS, Hur D et al (2010) Gentamicin-induced spiral ganglion cell death: apoptosis mediated by ROS and the JNK signaling pathway. Acta Otolaryngol 130(6):670–678

Katano H, Sato Y, Tsutsui Y, Sata T, Maeda A, Nozawa N, Inoue N, Nomura Y, Kurata T (2007) Pathogenesis of cytomegalovirus-associated labyrinthitis in a guinea pig model. Microbes Infect 9:183–191

Kim HJ, Lee JH, Kim SJ et al (2010) HS Roles of NADPH oxidases in cisplatin-induced reactive oxygen species generation and ototoxicity. J Neurosci 30:3933–3946

Kim SJ, Park C, Han AL, Youn MJ, Lee JH, Kim Y, Kim ES, Kim HJ, Kim JK, Lee HK, Chung SY, So H, Park R (2009) Ebselen attenuates cisplatin-induced ROS generation through Nrf2 activation in auditory cells. Hear Res 251:70–82

Kosugi I, Kawasaki H, Arai Y, Tsutsui Y (2002) Innate immune responses to cytomegalovirus infection in the developing mouse brain and their evasion by virus-infected neurons. Am J Pathol 161:919–928

Li L, Kosugi I, Han GP, Kawasaki H, Arai Y, Takeshita T, Tsutsui Y (2008) Induction of cytomegalovirus-infected labyrinthitis in newborn mice by lipopolysaccharide: a model for hearing loss in congenital CMV infection. Lab Invest 88:722–730

Livak KJ, Schmittgen TD (2001) Analysis of relative gene expression data using real-time quantitative PCR and the 2(−Delta Delta C (T)) Method. Methods 25:402–408

Low WK, Sun L, Tan MG, Chua AW, Wang DY (2008) L-N-Acetylcysteine protects against radiation-induced apoptosis in a cochlear cell line. Acta Otolaryngol 128:440–445

Marques CP, Cheeran MC, Palmquist JM, Hu S, Lokensgard JR (2008) Microglia are the major cellular source of inducible nitric oxide synthase during experimental herpes encephalitis. J Neurovirol 14:229–238

Matkovic S, Vojvodic D, Baljosevic I (2007) Comparison of cytokine levels in bilateral ear effusions in patients with otitis media secretoria. Otolaryngol Head Neck Surg 137:450–453

Micheau O, Tschopp J (2003) Induction of TNF receptor I-mediated apoptosis via two sequential signaling complexes. Cell 114:181–190

Muppidi JR, Tschopp J, Siegel RM (2004) Life and death decisions: secondary complexes and lipid rafts in TNF receptor family signal transduction. Immunity 21:461–465

Mutnal MB, Cheeran MC, Hu S, Lokensgard JR (2011) Murine cytomegalovirus infection of neural stem cells alters neurogenesis in the developing brain. PLoS One 6:e16211.

Nesin M, Cunningham-Rundles S (2000) Cytokines and neonates. Am J Perinatol 17:393–404

Ohinata Y, Miller JM, Altschuler RA, Schacht J (2000) Intense noise induces formation of vasoactive lipid peroxidation products in the cochlea. Brain Res 878:163–173

Ohinata Y, Miller JM, Schacht J (2003) Protection from noise-induced lipid peroxidation and hair cell loss in the cochlea. Brain Res 966:265–273

Otis EM, Brent R (1954) Equivalent ages in mouse and human embryos. Anat Rec 120:33–63

Park AH, Gifford T, Schleiss MR et al (2010) Development of cytomegalovirus-mediated sensorineural hearing loss in a Guinea pig model. Arch Otolaryngol Head Neck Surg 136:48–53

Satoh H, Firestein GS, Billings PB, Harris JP, Keithley EM (2002) Tumor necrosis factor-alpha, an initiator, and etanercept, an inhibitor of cochlear inflammation. Laryngoscope 112:1627–1634

Schachtele SJ, Hu S, Little MR et al (2010) Herpes simplex virus induces neural oxidative damage via microglial cell Toll-like receptor-2. J Neuroinflammation 7:35

Song L, McGee J, Walsh EJ (2006) Frequency- and level-dependent changes in auditory brainstem responses (ABRS) in developing mice. J Acoust Soc Am 119:2242–2257

Staczek J (1990) Animal cytomegaloviruses. Microbiol Rev 54:247–265

Stoddart CA, Cardin RD, Boname JM, Manning WC, Abenes GB, Mocarski ES (1994) Peripheral blood mononuclear phagocytes mediate dissemination of murine cytomegalovirus. J Virol 68:6243–6253

van Den Pol AN, Mocarski E, Saederup N, Vieira J, Meier TJ (1999) Cytomegalovirus cell tropism, replication, and gene transfer in brain. J Neurosci 19:10948–10965

Van Wijk F, Staecker H, Keithley E, Lefebvre PP (2006) Local perfusion of the tumor necrosis factor alpha blocker infliximab to the inner ear improves autoimmune neurosensory hearing loss. Audiol Neurootol 11:357–365

Wakabayashi K, Fujioka M, Kanzaki S et al (2009) Blockade of interleukin-6 signaling suppressed cochlear inflammatory response and improved hearing impairment in noise-damaged mice cochlea. Neurosci Res 66(4):345–352

Wang X, Truong T, Billings PB, Harris JP, Keithley EM (2003) Blockage of immune-mediated inner ear damage by etanercept. Otol Neurotol 24:52–57

Whitlon DS, Szakaly R, Greiner MA (2001) Cryoembedding and sectioning of cochleas for immunocytochemistry and in situ hybridization. Brain Res Brain Res Protoc 6:159–166

Yamashita D, Jiang HY, Schacht J, Miller JM (2004) Delayed production of free radicals following noise exposure. Brain Res 1019:201–209

Zine A, van de Water TR (2004) The MAPK/JNK signalling pathway offers potential therapeutic targets for the prevention of acquired deafness. Curr Drug Targets CNS Neurol Disord 3:325–332